

# Design of Miniature Bellow in a Conceptual Joule-Thomson Cooler

F. Can<sup>1</sup>, A. B. Erdogmus<sup>1</sup>, M. Baki<sup>1</sup>, M. K. Aktas<sup>2</sup>, M. A. Güler<sup>2</sup>

<sup>1</sup> Department of Mechanical Design, ASELSAN INC,  
MGEO Cankiri Yolu 7. Km Akyurt/Ankara/TURKEY

<sup>2</sup> Department of Mechanical Engineering, TOBB University  
of Economics and Technology, Ankara/TURKEY

## ABSTRACT

Flow control is an important issue in the solution of many engineering problems. Engineers may use different methods depending on the system size, energy consumption requirement, actuator type, etc. Since the gas source is limited in open cycle Joule-Thomson (JT) applications, the gas flow rate must be minimized to have a long operation time. When flow regulation is not considered, the flow cross sectional area in an expander must be made small in order to decrease the gas flow rate and thus extend operating time. But this situation also has some disadvantages because of the longer temperature drop time. In the literature, most of the JT coolers employ miniature bellows as a flow controller unit to maintain sustainability of the gas source. One end of these bellows, whose either inside or outside is filled with high pressure gas, is connected to a rod. The rod, which is also called as the sensing rod, is in contact with the gas liquefied by the Joule-Thomson effect. Temperature information on the liquefied gas is sensed and transmitted through the walls of the bellows to the interior of the bellow which is filled with high pressure gas. The pressure of gas inside the bellow drops while the temperature decreases. The motion of the sensing rod causes the flow cross-sectional area to decrease as a result of the temperature decrease. The length and cold side temperature of the JT cryocooler affects the bellow's surface temperature distribution, thus its internal pressure. In this study, the contraction of the bellow due to temperature decrease is investigated in a numerical way for different lengths and cold side temperatures.

## INTRODUCTION

Expansion or contraction of materials is generally undesirable in engineering designs. Only tolerated displacements of materials are acceptable. However some kinds of displacements in materials may be useful when flow control with respect to flow temperature is needed. Minimizing excessive mass flow rate of cryogenic gas is the objective of a flow control unit in Joule-Thomson cryocoolers. Therefore, the flow control unit is one of the important components of advanced open cycle Joule-Thomson cryocoolers.<sup>1</sup> Without flow control, the cooler is designed either with a low flow rate, which is required for steady state and the temperature drop time is long, or it is designed with a high flow rate, which is required to have short temperature drop time; but the operating time of the cooler becomes shorter. The control mechanism is designed in order to use a limited gas source effectively. For this purpose, different types of control mechanisms can be used in Joule-Thomson coolers. In this application, it is observed that miniature bellows with different dimensions have been used frequently. Flow control can also be implemented utilizing bimetal materials

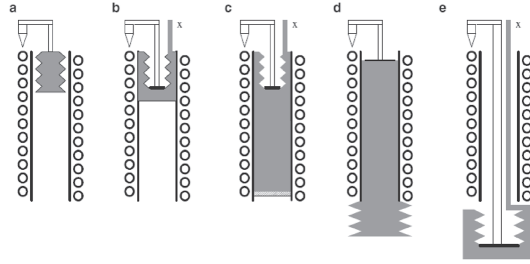


**Figure 1.** Different type of pressurized bellow using in JT cryocoolers<sup>2</sup>.

that depend on the differences in expansion properties of two combined materials. These materials have a simple design. Since the spring rate of bimetals are higher, they may withstand higher drag forces and the cold end temperature stability is higher than bellows. Also, the thermal mass of bimetals is larger than bellows.<sup>1</sup> As a result, the temperature fluctuation is less, and the gas consumption is also lower. In spite of these advantages of bimetals, bellows are preferred in commercial products because of having faster response time. In addition, bellows are less sensitive to clogging.<sup>2</sup>

Bellows are generally produced by special coating techniques because of having small dimensions. This production method is known as electroforming. It is expensive, especially for very small sized bellows. It also includes a needle valve and a rod. When gas begins to liquefy, the rod attached to the bellow senses the liquefying temperature. From this time until full contraction of the bellows can be called the bellows response time. It changes between 5 to 10 seconds.<sup>1</sup> Bellows can be positioned at cold side (as shown in Figure 1 a, b and c) or hot side (as shown in Figure 1 d and e). Bellows can be pressurized from inside (as shown in Figure 1 a and d) or outside (as shown in Figure 1 b, c and e).<sup>2</sup> Since there is a sensing rod attached to the bellow, the thermal mass changes depending on the location of the rod. For a flow control unit with a long sensing rod, as long as shown in Figure 1 e, the thermal mass of the cooler will be high. It can be useful if the length of the cooler is very short.<sup>2</sup>

It is found that most of the studies in the literature on JT coolers do not focus on the flow control. Chien et al.<sup>4,5</sup> studied a Joule-Thomson cryocooler with a bellow flow control mechanism. Nitrogen gas is used as the working gas in their research, and the cryocooler includes a miniature bellows pressurized with nitrogen. Chien<sup>4,5</sup> not only studied the behavior of the bellow but also solved the effect of other components. In the Chien study<sup>3</sup>, the cooling time of a cryocooler, which does not involve any flow control unit, is investigated experimentally and theoretically. In their other study<sup>4</sup>, cooling time and the change in mass flow rate of a JT cryocooler with a flow controller is examined. It is obvious that the temperature of the gas outside the mandrel or bellow has an important effect on the determination of bellows behavior. A remarkable difference between the first<sup>3</sup> and second<sup>4</sup> studies is examination of different orifice structures. In their second study<sup>4</sup>, the mass flow rate is decreased 95 percent with regard to its initial value. It is noted that with a cryocooler with a flow controller, the operation time can be 20 times increased after reaching a steadystate condition. In another study of Chien<sup>5</sup>, the condensation of the gas inside the bellow is taken into consideration and a sudden pressure drop is observed at the condensation point. They determined that the amount of contraction of bellows is higher when condensation is considered. It is validated that modelling condensation has an important effect on the design of a flow control unit. In addition, the effect of the rigidity of the bellows on contraction rate is researched. The heat transfer is considered between the bellow and cold end because of contact. But the heat transfer between bellow and mandrel at the hot side is ignored. In their research<sup>3</sup>, the temperature of the contact region between the bellow and the mandrel at the hot side is above 200 K. Therefore, a considerable amount of heat is transferred from this region. Their studies<sup>4</sup> demonstrate that the temperature distribution is between 83 and 90 K at the steadystate condition. It can be noted that the temperature range is wide in the real case because of the contact between bellow and mandrel at the hot side.

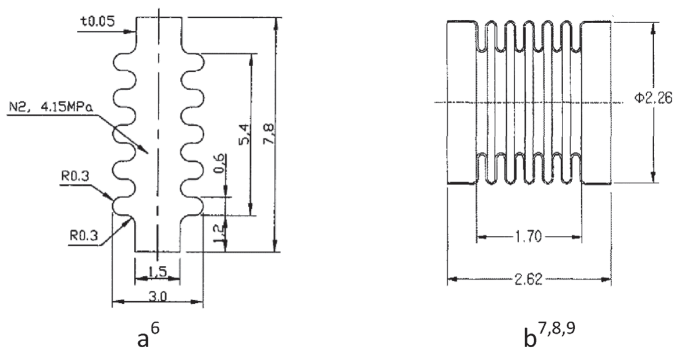


Figure 2. Bellow dimensions in Lee's studies<sup>6,7,8,9</sup>.

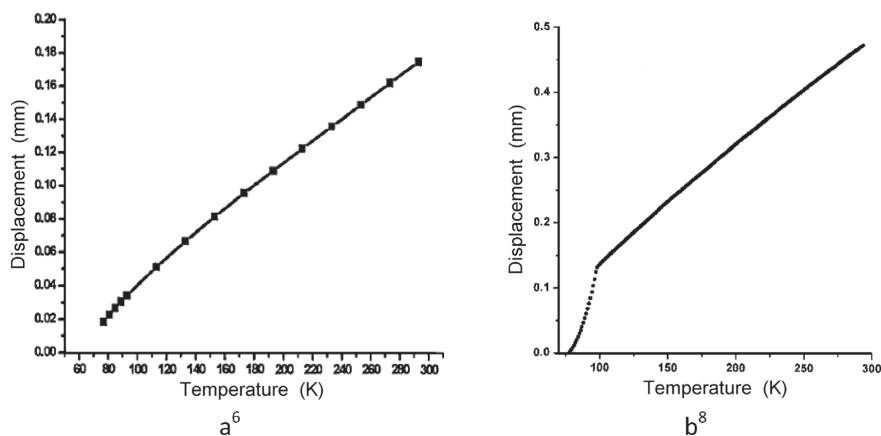


Figure 3. Axial deformation of bellows in Lee's studies<sup>6</sup>.

Another series of studies was performed by Lee, et al.<sup>6,7,8,9</sup> In those studies, only pressurized bellows were examined, and the contraction and expansion of the bellow due to different pressures and temperatures of gas were determined experimentally and numerically. The dimensions of bellows used in their studies are given in Figure 2.

The only available numerical analysis is for the bellow given in Figure 2 a. In that study<sup>6</sup>, the pressure drop depends on the temperature decrease in nitrogen gas and is modelled by the BWR method, and then the contraction of the bellow is calculated. In their other research<sup>7</sup>, the bellows shown in Figure 2 b is used. Different pressures are tried for the same temperature, and the amount of contraction is calculated for different points. Deformation analysis is performed by a commercial finite element code ANSYS. The bellows are modeled by 3-node axisymmetric shell elements with reduced integration. Finally, experiments were performed to validate the conducted numerical analyses with experimental values. In another study<sup>8</sup>, the dependency of pressure drop on temperature was researched similar to their first study. The only difference stems from the gas model. The Modified Benedict Webb Rubin (MBWR) method was used in that study. When results are interpreted, it is seen that the deformation in the study<sup>6</sup> is nearly linear, since the BWR model does not reflect the phase change in gases as shown Figure 3 a. However, the MBWR method models the two phase region more accurately as compared to the BWR method. Therefore, nonlinear deformation is seen below the condensation temperature as shown Figure 3 b. Finally, they conducted an experimental study to support their last research.<sup>9</sup>

**Table 1.** Bellow dimensions

	Value (mm)
Inner diameter ( $d_{bi}$ )	2.2
Outer diameter ( $d_{bo}$ )	2.3
Thickness ( $t_b$ )	0.025
Length ( $L_b$ )	10
Number of pitch ( $N_b$ )	10

**DEFORMATION ANALYSES**

In this article, a bellow is studied as a flow control unit. Displacement of the bellow mainly arises from an internal pressure change. Also, a temperature decrease causes a desired movement in the bellow in addition to changing its pressure. As with the bellow, the temperature of the mandrel also decreases. The thermal expansion coefficient of the bellow and mandrel materials also affects the contraction due to the temperature drop. When the pressure drop of the gas as a result of temperature decrease is also taken into consideration, superposition of these two effects fulfills the function of the flow control unit. Flow restriction is accomplished by the rod which senses the liquefaction temperature at the exit pressure of the high pressure gas. The rod is attached to the cold side of the bellow. When liquefaction is accomplished, the needle moves with the rod towards the orifice. In this study, displacement in the bellow is modelled by numerical methods in three steps: analysis performed by in-house code, commercial finite element, and finite volume solvers (ANSYS and FloEFD).

In the first step, since three dimensional models and real gas models of Argon are complicated, the temperature distribution on the mandrel is calculated with a numerical approach. The MBWR<sup>11</sup> method based on NIST data is used to model the real gas. In-house code written in MATLAB is developed to solve the differential equations using a finite difference method.

Bellows with different pressures can be utilized in real applications. Therefore, the effect of inside pressure is studied to understand the behavior of the bellows. The temperature distribution and internal pressure of the gas under steadystate conditions are solved in step 2. The temperature distribution of the mandrel, which is the result of the first step, is used as a boundary condition. To define the gas inside the bellow, the default real gas model of nitrogen in FloEFD is used. When iteration times are taken into consideration, the first and second steps are completed in 30 and 150, respectively.

The calculated final pressure value is used in the next step. The bellow stiffness is calculated for the dimensions presented in Table 1. Since FloEFD is not used for structural analysis, finite element software ANSYS R 15 is preferred to calculate the displacement in the bellow. A 2D axisymmetric model with PLANE 183 as a discretization element is used. PLANE 183 has a quadratic displacement behavior and is suited for modeling irregular meshes. Pressure is defined as a surface load. PLANE 183 elements are defined by 8 nodes.

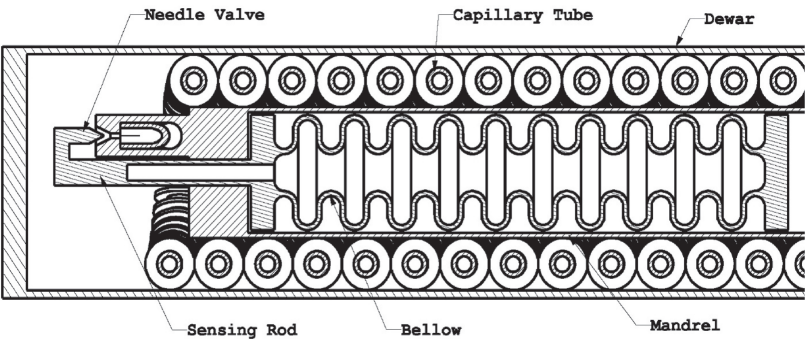


**Figure 4.** Three dimensional schematic model of JT

Table 2. Other dimensions

	Value (mm)
Length of JT (L)	50
Pitch of helical coil ( $P_c$ )	1
Pitch of fin ( $P_f$ )	0.3
Mean diameter of helical coil ( $D_{hel}$ )	3.5
Fin diameter ( $d_f$ )	1
Fin thickness (t)	0.1

Table 3. Main dimensions

	Inner Diameter (i) (mm)	Outer Diameter (o) (mm)
Capillary tube ( $d_c$ )	0.3	0.5
Mandrel( $d_m$ )	2.3	2.5
Shield (Dewar)( $d_s$ )	4.5	4.8

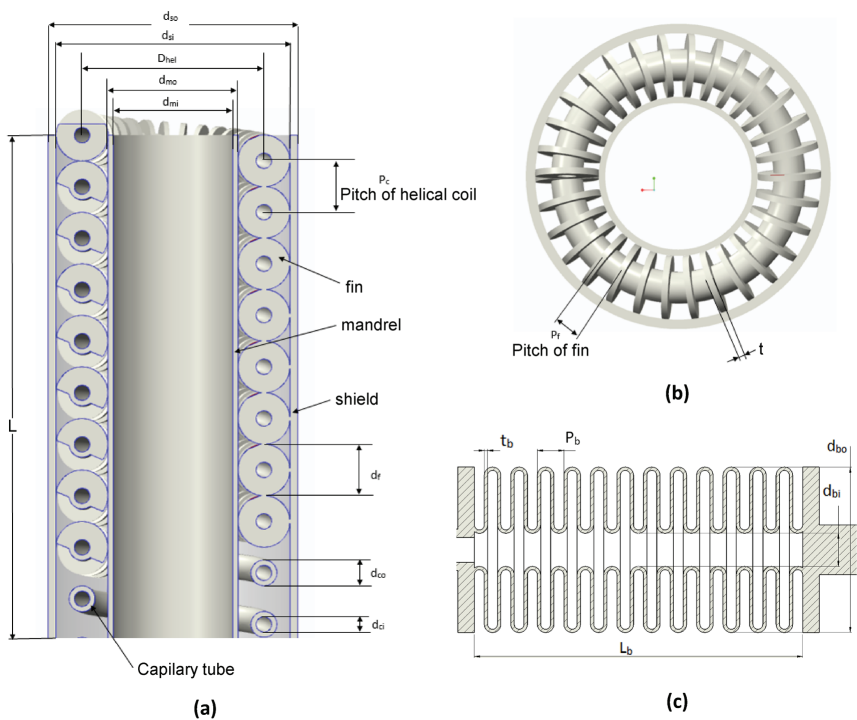


Figure 5. Schematic view of dimensions used in analysis

Models

A sectional view of whole system is demonstrated schematically in Figure 4. The cold side is located at the left side in this figure. The hot side of the bellow is assembled to the mandrel at the right side.

In Figure 5, details of the parameters used in the numerical calculations are given. Figure 5a and b show important parameters used in the first step calculations. Parameters shown in the cross-sectional view of the bellow (Figure 5 c) are input design values and used in dimensions given in the second and third steps. All dimensions used in the solution of the problem are presented in Table 1 - 3. The 3D model shown in Figure 5 is simplified to a 1D model with 500 nodes in the first step. In the second step, the three dimensional problem is solved with 570,000 cells. In the final step, the problem is solved with 130,000 elements.

**Table 4.** Boundary Conditions

Step	Location	Boundary Conditions
1	x=0	$T_{h,1} = T_{h,in}, \frac{dT_s}{dx} = 0, \frac{dT_w}{dx} = 0, \frac{dT_m}{dx} = 0, P_{h,1} = P_{h,in}$
	x=L	$T_{c,imax} = T_{c,in}, \frac{dT_s}{dx} = 0, \frac{dT_w}{dx} = 0, \frac{dT_m}{dx} = 0, P_{c,imax} = P_{c,in}$
2	x=0	$T_{m,in}$
	x=L	$T_{m,out}$
	$0 \leq x \leq L$	Temperature Distribution on Mandrel
3	-	Internal Pressure

**Table 5.** Equations used in the calculations

Name	Equations
Continuity	$\frac{d\dot{m}}{dx} = 0$
Momentum equations	$\frac{dP}{dx} = -\rho \cdot V \left( \frac{dV}{dx} + 2 \cdot \frac{fV}{d} \right)$
Hot fluid energy	$\dot{m}_h C_{ph} \frac{dT_h}{dx} = h_h p_h (T_w - T_h)$
Cold fluid energy	$\dot{m}_c C_{pc} \frac{dT_c}{dx} = h_c [p_c (T_c - T_w) + p_{si} (T_c - T_s) + p_{mo} (T_c - T_m)]$
Capillary Tube energy	$k_w A_w \frac{d^2 T_h}{dx^2} = h_h p_c (T_h - T_w) + h_c p_c (T_c - T_w)$
Mandrel	$k_m A_m \frac{d^2 T_s}{dx^2} = h_c p_{mo} (T_c - T_m)$
Dewar (Shield)	$k_s A_s \frac{d^2 T_s}{dx^2} = h_c p_{si} (T_c - T_s) + \sigma p_{so} (T_a^4 - T_s^4)$

**Table 6.** Other equations

Fanning friction factor for Hot fluid <sup>2</sup>	$f = 0.046 \left( 1 + \frac{3.5 d_{ci}}{D_{hel}} \right) Re^{-0.2} \text{ for } Re > 30000$
Cold fluid Fanning friction factor <sup>10</sup>	$f = (0.088 + 0.16 X_L (X_T - 1)^{-n}) \frac{2}{Re^{0.15}}$
Hot fluid heat convection <sup>10</sup>	$h = 0.023 C_{ph} G \left( 1 + \frac{3.5 d_{ci}}{D_{hel}} \right) Re^{-0.2} Pr^{-2/3} \text{ for } Re > 10000$
Cold fluid heat convection <sup>10</sup>	$h = 0.26 C_{pc} G Re^{-0.2} Pr^{-2/3}$

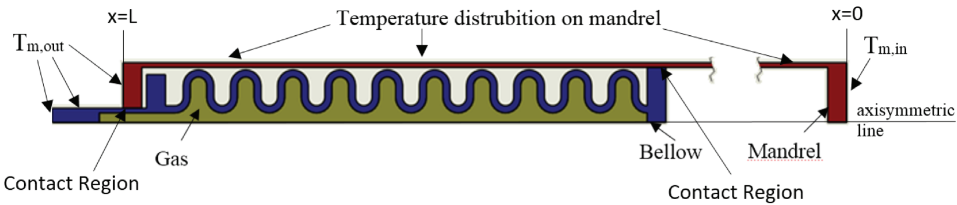


**Figure 6.** Boundary conditions and axisymmetric model of Step 2

**Table 7.** Material specification of nickel used in FEM analysis<sup>12</sup>

Property	Value
Young modulus (MPa)	160992
Position ratio	0.28
Yield strength (MPa)	754.8
Tensile strength (MPa)	861.8

**Table 8.** Comparison of numerical solution of Step 1 (L=50mm) with experimental data<sup>13</sup>

Pressure (bar)		Temperature(K)		Mass flow (SLPM)	Temperature(K) (T <sub>c_out</sub> )	
P <sub>h_in</sub>	P <sub>c_in</sub>	T <sub>h_in</sub>	T <sub>c_in</sub>		Experiment <sup>12</sup>	Simulation
140.47	1.3426	291.94	90.06	10.145	284.98	285.01

Details of Analyses

The surface temperature distribution of the mandrel is found in the first step for steadystate conditions. In this step, boundary condition 1 in Table 4 is used to solve the continuity, momentum and energy equations given in Table 5. To solve the momentum and energy equations needs friction factors and heat transfer coefficients; equations for Fanning friction factors and heat transfer coefficients are required. Coefficients used frequently in the literature are given in Table 6.

Boundary conditions and the contact region between mandrel and bellows for the second step analysis are shown in Figure 6. Nickel whose material specifications<sup>12</sup> are detailed in Table 7 are used as the bellow material in the third step.

RESULTS AND DISCUSSION

In this section, results obtained in the three steps are summarized and some of them compared with the results published in the literature. In the first step, the problem is solved with the same boundary conditions and geometry studied by Chua et al.<sup>13</sup> In Table 8, the first five columns are input values for the presented numerical study. In the last two columns, experimental data for the cold fluid outlet temperature are compared with numerical results. It is seen that the two values are very close to each other. Also, this simulation is repeated with different conditions presented in the study of Chua et al.<sup>13</sup> Similar results are determined for other conditions. After that, the temperature distribution of the mandrel is calculated for different heat exchanger lengths and different cold end temperatures as illustrated in Figures 7 and 8. These results are used as a boundary condition for the second step in the calculation of the final pressure of the gas inside the bellow.

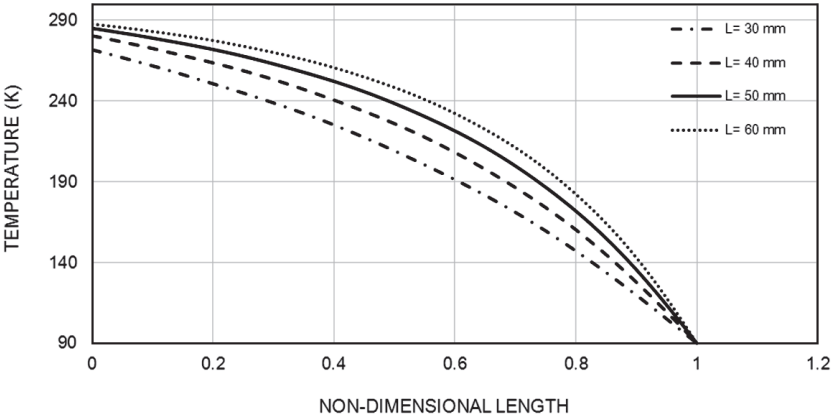


**Figure 7.** Temperature change along the mandrel in different heat exchanger length (Step 1)

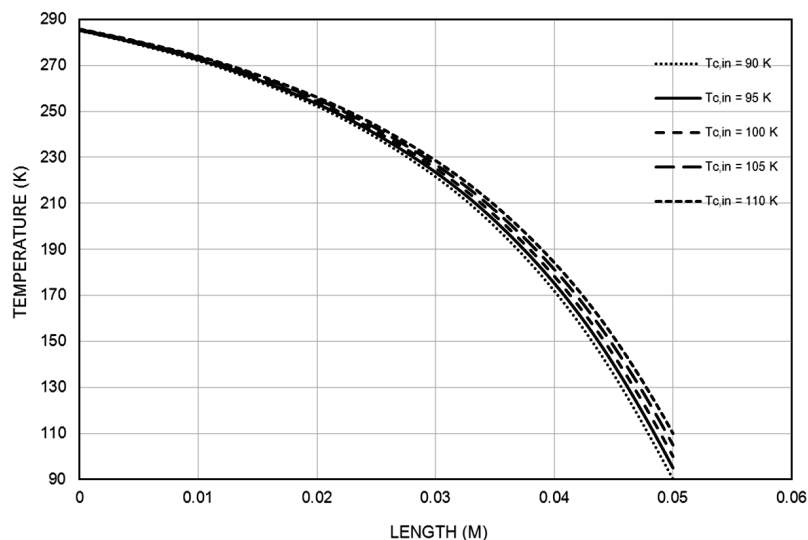


**Figure 8.** Temperature distribution in different cold side temperatures ( $L=50\text{ mm}$ , Step 1)

**Table 9.** Temperature distribution and internal pressure of gas in steady state condition for different length heat exchanger.  $P_{\text{gas},0}=30\text{ bar}$  (at  $295\text{K}$ ),  $T_{\text{c},\text{in}}=90$ .

$L$ (mm)	$T_{\text{gas},f}(\text{K})$	$P_{\text{gas},f}(\text{bar})$
30	$90 < T < 184.35$	11.63
40	$90 < T < 179.72$	11.46
50	$90 < T < 177.33$	11.37
60	$90 < T < 175.91$	11.31

**Table 10.** Temperature interval, internal pressure of gas and deformation of bellow in steady state condition for different initial internal pressure ( $L=50\text{ mm}$ ,  $T_{\text{c},0}=90$ ).

$P_{\text{gas},0}(\text{bar})$	$T_{\text{gas},f}(\text{K})$	$P_{\text{gas},f}(\text{bar})$	$\Delta x\text{ (}\mu\text{m)}$
20	$90 < T < 177.34$	7.98	93.8
25	$90 < T < 177.34$	9.70	119.4
30	$90 < T < 177.33$	11.37	145.3
35	$90 < T < 177.33$	12.93	172.2

The final pressures and gas temperatures in the bellow, which is calculated in the second step, are given in the third column of Table 9. Bellow stiffness is calculated as 128.18 Bar/mm in the third step. Initial pressure of gas inside the bellow should be lower than 37.2 bar for safety operation of the bellow. This is the buckling pressure for the investigated bellow. With the calculated stiffness factor and final pressures, the deformations shown in Table 10 are calculated.

Evaluation of results are listed below.

- Temperature distribution of gas inside the bellow covers large interval when it is compared with the results given in the literature.
- The heat transfer at the hot side of bellow has important effect on inside pressure of bellow.
- The bellow should be well isolated from the hot side of the mandrel to prevent local heat transfer
- The results of this study may be taken into consideration in orifice design
- Buckling pressure should be taken into consideration in design of operating conditions. If the pressure is greater than buckling pressure, the bellow can lose its functionality.



- Needle attached to bellow moves a maximum of 172  $\mu\text{m}$  with the presented bellow dimensions. This result should be taken into consideration in orifice design.

## REFERENCES

1. Buelow, P.L., Ryba, E.L., Skertic, M.M., "Fast Response Joule-Thomson Cryostat", US Patent Application Publication No. US 5,913,889, filed August 20, 1996, published June 22, 1999, Hughes Electronics, Los Angeles, California.
2. Maytal, B.Z., Pfotenhauer, J.M., *Miniature Joule-Thomson Cryocooling*, Springer, New York (2013), p. 73, 220,225.
3. Chou, F.C., Pai C.F., Chien, S.B., Chen J.S., "Preliminary Experimental and Numerical Study of Transient Characteristics for a Joule-Thomson Cryocooler," *Cryogenics*, vol. 35 (1995), p. 311-316.
4. Chien, S.B., Chen, L.T., Chou, F.C., "A Study on the Transient Characteristics of a Self-Regulating Joule-Thomson Cryocooler," *Cryogenics*, vol. 36, no. 12 (1996), pp. 979-984.
5. Chou, F.C., Chien, S.B., "Two-phase coexistence analysis of the Bellows Control Mechanism for a J-T Cryocooler", *Cryogenics*, vol. 39 (1999), pp. 359-365.
6. Lee, S.E., Lee, T.W., "Deformation Analysis of Self-regulating Bellows in Joule-Thomson Cryocooler," *Journal of the Korean Society for Precision Engineering*, vol. 25, no. 4 (2008).
7. Lee, S.E., Lee, T.W., "A Study on the Structural Characteristics of Miniature Metal Bellows in Joule-Thomson Micro-Cryocooler," *Journal of the Korean Society for Precision Engineering*, vol. 25, no. 9 (2008).
8. Lee, S.E., Lee, T.W., "Deformation Analysis of Miniature Metal Bellows Charged Nitrogen for Temperature Change to Cryogenic Condition," *Journal of the Korean Society for Precision Engineering*, vol. 26, no. 10 (2009), pp. 81-88.
9. Lee, S.E., Lee, T.W., "Study on Deformation of Miniature Metal Bellows in Cryocooler Following Temperature Change of Internal Gas," *Transactions of the Korean Society of Mechanical Engineers*, vol. 39, no. 4 (2015), pp. 429-435.
10. Timmerhaus, K.D., Flynn, T.M., *Cryogenic Process Engineering*, Springer, New York (1989), p. 194-198.
11. Younglove, B.A., "Thermophysical properties of fluids 1 Argon, Ethylene, parahydrogen, nitrogen, nitrogen trifluoride, and oxygen," *Journal of physical and chemical reference data* 11(1), (1982) pp 1-8.
12. Servometer company, "Electroformed Metal Bellows Catalog," Servometer.com
13. Chua, H.T., Wang, X., Teo, H.Y., Ng, K.C., "A Numerical Study of the Hampson-Type Joule-Thomson Cooler," *Int. Refrigeration and Air Conditioning Conference* 2004, pp. R149-1.